

Understanding gravity gradiometry processing and interpretation through the Kauring test site data

Cercia Martinez
Colorado School of Mines
cemartin@mines.edu

Yaoguo Li
Colorado School of Mines
ygli@mines.edu

SUMMARY

The Kauring Gravity Gradiometry Test site offers a unique opportunity to understand the information content of various types of gravity gradient measurements and the required processing and interpretation techniques. In this paper, we utilize the measured ground vertical gravity data to simulate realistic airborne gravity gradiometry data from several current and future systems using an equivalent-source technique. We then invert these simulated data for the underlying density contrast and evaluate the performance of these inversions. The study demonstrates the effectiveness of equivalent-source based method for data conversion in the presence of scattered observations. The major density features recovered from the optimally converted gradient data are highly consistent with those from the original ground gravity.

Key words: Gravity gradiometry, inversion, interpretation, Kauring Test Site.

INTRODUCTION

With the technological advancements in gravity gradiometry instrumentation, there is a need for understanding both the information content of modern gravity gradiometry data relative to traditional gravity data, and for developing processing and interpretation tools that assess the myriad of measured gradient components and information they contain. The Kauring Airborne Gravity Gradiometry Test Site and associated data provide a unique and important opportunity to address these two aspects and to explore the applicability of existing tools.

In this study, we focus on the available gravity data acquired from a ground survey and carry out investigations in anticipation of the availability of acquired gradiometry data from different systems.

We first examine the signature of airborne gravity gradients due to the density structure below the test site. From the observed ground gravity data, we calculate full tensor gravity gradient data and typical components from newer gradiometer systems in development by using a regularized equivalent source method. These derived gravity gradient data are then subjected to appropriate low-pass filtering to simulate realistic data. The converted data sets may serve as a reference for comparison with the acquired data in the future. Secondly, we then interpret the simulated data sets by inverting various components for 3D density contrast distributions and perform quantitative evaluations.

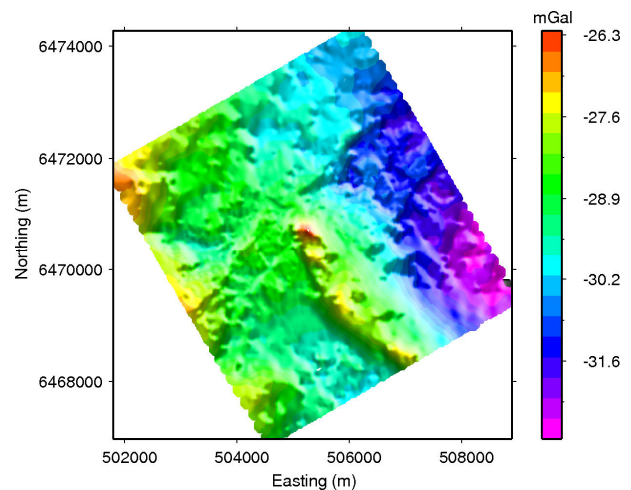


Figure 1. Ground gravity in the airborne gravity gradient area of the Kauring test site

The information content of these data sets are assessed through the recovered density models in comparison to that obtained from the inversion of ground gravity data.

GRAVITY GRADIENT FROM GROUND GRAVITY

The ground vertical gravity data were acquired for the explicit purpose of establishing the reference for assessing airborne gravity gradient data to be acquired above the Test Site (Geoscience Australia, 2010). The gravity data available from the website for the Test Site are shown in Figure 1. Observation lines are oriented northeast to southwest, with progressively greater station spacing moving out from the centre of the data. The data shows a focused anomaly high in the centre and a broad linear feature to the southeast. There is also a regional field trending east-west.

We examine the associated gravity gradiometry responses and their ability to characterize the high-density anomaly beneath the test range. To simulate the gradient data that would be acquired by airborne systems, we use a regularized equivalent source technique to convert the ground gravity data to gravity gradient components. The approach has the benefit of attenuating data error and producing more reliable gradients. There is also a negative DC in the data.

The equivalent source layer is composed of 100-m cubic cells located 100 m below the lowest observation point and we use a regularized inverse approach to determine the density values in the layer. An L-curve criteria (Hansen, 1992) was used to select the optimal regularization level so that the calculated gradient components are minimally affected by the noise in the ground gravity data.

The constructed equivalent source layer is shown in Figure 2. The equivalent source method used in our processing achieves two benefits. First, it attenuates data error due to the ability of the equivalent source layer to optimally misfit data according to the noise level. Secondly, it also allows the removal of a regional trend so the calculated gravity gradients are consistent with the targets.

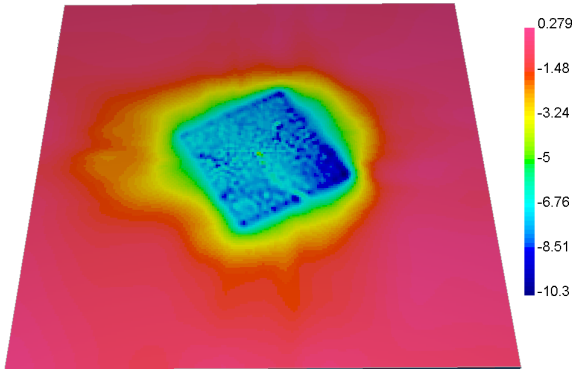


Figure 2. Equivalent source layer generated using ground gravity data.

From the equivalent source layer, we first calculated the five independent components along with T_{zz} (referred to as six-component data). We then combine these components to form the specific data quantities measured by different systems. For example, two components measured by Rio Tinto's VK1 system (Anstie, 2010) are given by

$$\begin{aligned} vka &= T_{zz} - T_{aa} \\ vkc &= T_{zz} - T_{cc} \end{aligned} \quad (1)$$

where T_{aa} is the diagonal component of the gradient tensor in the along-line direction and T_{cc} is the component in the cross-line direction. To obtain the two components T_{aa} and T_{cc} associated with an arbitrary flight direction, we apply a component rotation from the geographic coordinate system to the system affixed to the flight line direction.

In order to simulate realistic acquisition of gravity gradient data, a 4th order Butterworth filter was used to approximate the low-pass acquisition filter. The application of this filter serves to maintain a realistic level of processing before the data, and resulting signal, is inverted. The data was calculated with a constant drupe height of 150 m above the topographic surface. For brevity, we choose not to produce the six components here. We show the filtered vka and vkc for two different surveys in the central data area.

Figure 3 shows the data from a survey with a north-south heading (0° from the north) with 200-m line spacing and 30-m station spacing along lines. Figure 4 shows the corresponding vka and vkc data with a flight heading of 60° from north with line spacing matching that of the ground gravity data. Both of these configurations capture the target anomaly. We observed that the characteristics of vka and vkc anomalies switch between the two when the heading changes from 0° to 60° . The two main anomalies in the 0° vkc component show elongation oriented northwest to southeast, just as the 60° vka component. The 0° vka and 60° vkc have a distinctly more

circular appearance to the two anomalies. By examining these two configurations, we see how the information content of each component varies based on the line direction.

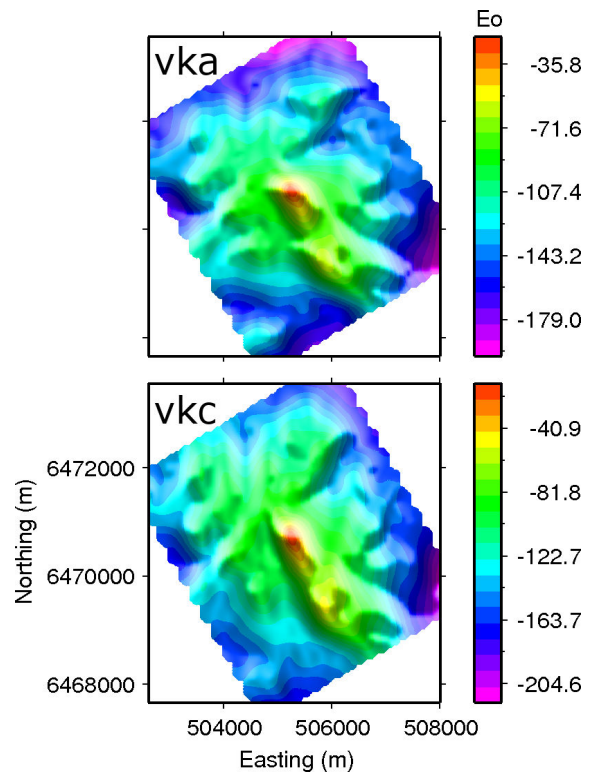


Figure 3. Calculated vka and vkc components from the equivalent source layer in Figure 2. The heading direction is assumed to be 0° from North.

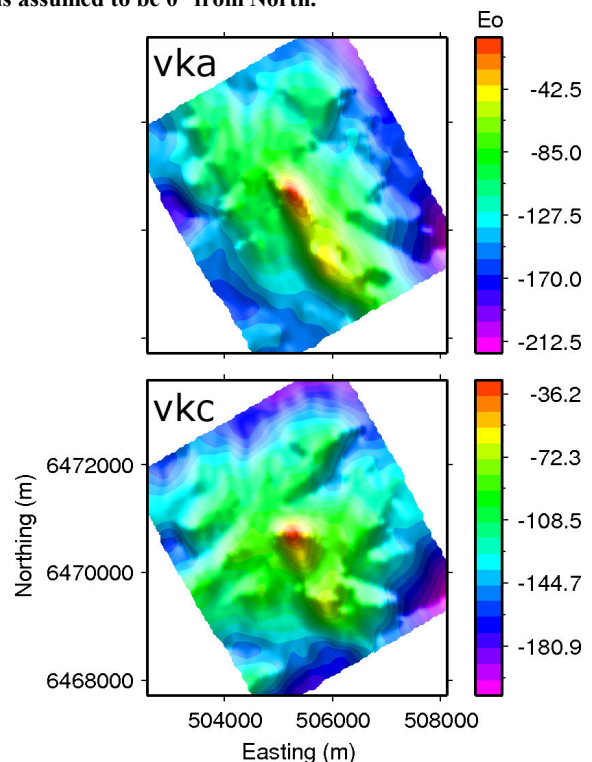


Figure 4. Calculated vka and vkc components with a flight heading of 60° from North.

INVERSION OF GROUND GRAVITY DATA

The ground gravity data is first inverted for a preliminary 3D density contrast distribution. The model obtained provides a basis for understanding the information contained within the gravity gradient components. The mesh used is composed of rectangular prisms with density contrast being constant within each cell. The mesh uses cuboidal cells of 50 m by 50 m by 50 m within the core of the data area and with increasing cell sizes towards the edges of the survey area and at depth. The rectangular mesh has cell dimensions of 132 cells in the easting, 136 cells in the northing, and 50 cells in depth giving a total of 897600 cells.

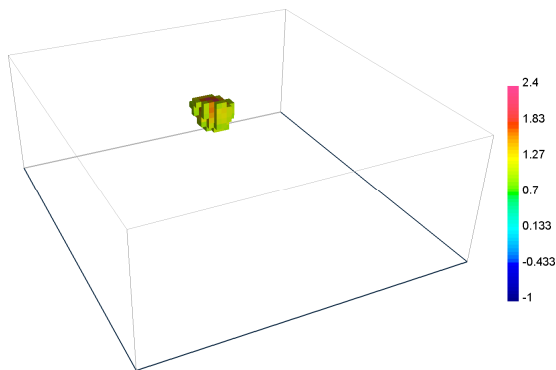


Figure 5. Volume rendered image of the 3D density contrast model (g/cc) constructed from ground gravity data with values less than 1 g/cc removed.

The ground gravity data was blindly inverted using a zero initial model and a zero reference model. A volume rendered image of the resulting model is shown in Figure 5 with all cells less than 1 g/cc removed for clarity. Note the positive density contrast feature in the middle of the model corresponding to the gravity high.

INVERSION OF GRAVITY GRADIENT DATA

To explore the information content of various gravity gradient components, we invert v_{ka} , v_{kc} , and the six component data separately. The v_{ka} and v_{kc} components were inverted using two different line headings of 0° and 60° from north. The five models were obtained using the same mesh discretization as that of the ground gravity inversion.

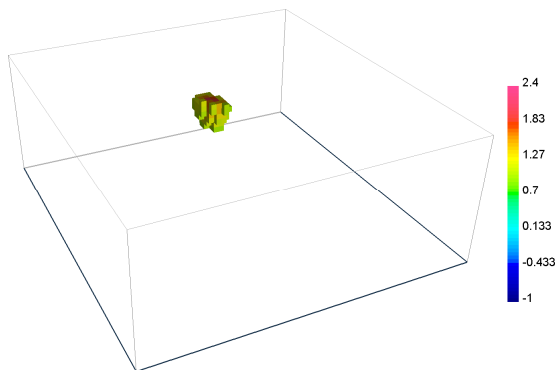


Figure 6. Volume rendered image of the 3D density contrast model (g/cc) constructed from six component data with values less than 1 g/cc removed.

Data from 0° heading

The three models were obtained through inversions using no prior geologic knowledge of the site. A zero reference model and zero initial model were used. The lower and upper bounds placed on the density contrast are -5.0 g/cc and 5.0 g/cc, respectively.

We first invert the full tensor data to obtain a density contrast distribution. A series of inversions using a range of regularization parameter values were carried out in order to determine the optimal parameter. In determining this parameter, we also gain insight into the noise content of the data by examining what part of the data signal the optimal model is unable to fit. We do not reproduce the predicted and difference data maps here for brevity. The standard deviation calculated from the difference maps is less than 1 Eo. It should be noted that the calculated data were subjected to two levels of noise reduction through the equivalent source construction and the applied filter to simulate the acquisition filters.

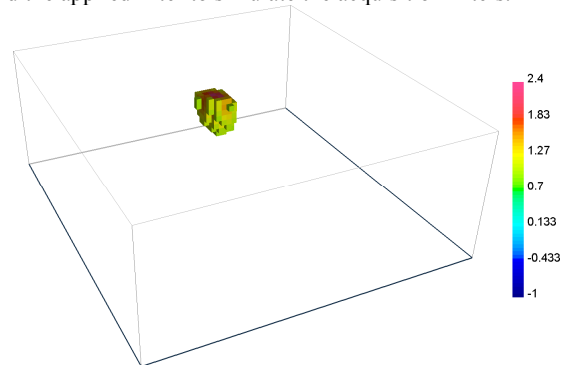


Figure 7. Volume rendered image of the 3D density contrast model (g/cc) constructed from v_{ka} (0° heading) data with values less than 1 g/cc removed.

A volume rendered image of the density contrast model is shown in Figure 6 with all cells below 1 g/cc removed in order to see the structure associated with the central anomaly.

Second, we invert v_{ka} using the same mesh and inversion parameters as the six component data. The data errors are estimated in the same manner as previously described with less than 1 Eo estimated. The density contrast volume resulting from inverting v_{ka} is shown in Figure 7 with a cut-off value of 1 g/cc.

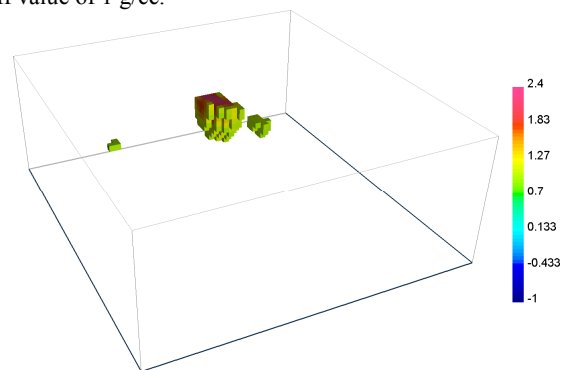


Figure 8. Volume rendered image of the 3D density contrast model (g/cc) constructed from v_{kc} data (0° heading) with values less than 1 g/cc removed.

Lastly we invert v_{kc} with the same mesh and inversion parameters. Data errors were estimated to be less than 1 Eo using the same methodology. The density contrast volume is displayed in Figure 8 with cells below 1 g/cc removed.

A singular dense feature corresponding to the gravity high is consistently seen in the three models. With a lower cutoff value, we see a less dense feature to the south. The structure seen within the three models is consistent with the model obtained from inverting the ground gravity data.

Data from 60° heading

We next invert the data with a more realistic flight line direction of 60° from north. This is more consistent with the layout of the airborne ground gravity Kauring test site. Without being verbose, the same mesh, initial model, reference model, and bound constraints were used for inversion of v_{ka} and v_{kc} with this new heading. The volume rendered image of the density contrast model resulting from inversion of v_{ka} is shown in Figure 9 with cells below 1 g/cc removed. The volume rendered image of the density contrast model resulting from inversion of v_{kc} is displayed in Figure 10 with cells below 1 g/cc removed.

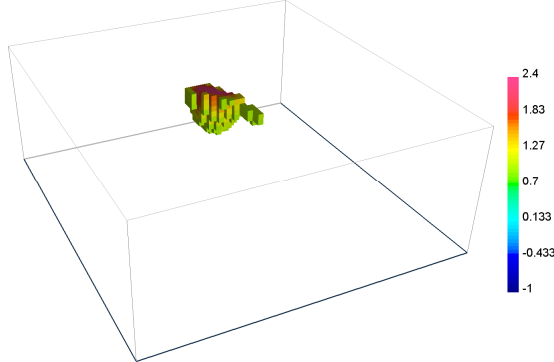


Figure 9. Volume rendered image of the 3D density contrast model (g/cc) constructed from v_{ka} data (60° heading) with values less than 1 g/cc removed.

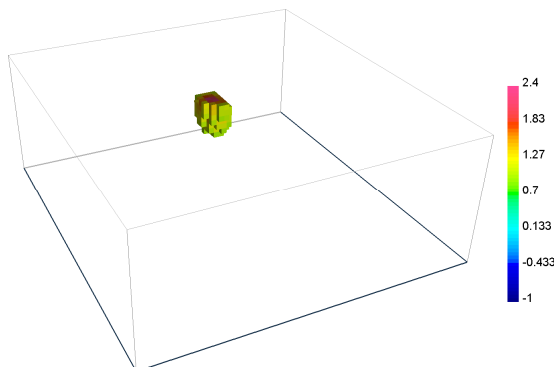


Figure 10. Volume rendered image of the 3D density contrast model (g/cc) constructed from v_{kc} data (60° heading) with values less than 1 g/cc removed.

Comparison with ground gravity inversion

The various gravity gradiometry inversions are highly consistent with the ground gravity inversion. All models recover a positive density contrast feature associated with the observed gravity high. Though not properly conveyed with the volume-rendered images used, all gravity gradient component models do recover a smaller positive density contrast feature

to the south of the main feature. The presence of this smaller feature again agrees with the ground gravity model and can be seen in the inversion of v_{ka} with 60° heading and v_{kc} with 0° heading.

CONCLUSIONS

We have used the ground vertical gravity data at the Kauring Test Site to simulate airborne gravity gradiometry data and investigated the information content through inversions. The use of regularized equivalent source construction proves to be a reliable tool for conversion and this approach should serve well in comparing gradient data to be acquired in the future with the ground gravity data.

For the main density anomaly seen at the Kauring Test Site, all inversions of simulated gradient data sets have produced consistent models, indicating that the particular example of data components and orientation used in the study are equivalent in information content. The variations in these density contrasts are representative of the varying information contained among individual components.

Compared with the density model from ground gravity data, these models from simulated gradient data appear to lose details and small-scale features. This difference indicates the loss of high-frequency information due to the increased observation height and low-pass filtering. However, overall structural features are in agreement through all models. Therefore, this may provide a basis for assessing the quality and information content of acquired gradiometry data at the Test Site in the future.

ACKNOWLEDGMENTS

We would like to thank Theo Aravanis and Bob Smith for helpful discussions on the VK1 system and the processing and inversion of VK1 data. We gratefully acknowledge the researcher, agencies, and companies who established the Kauring test site and made the associated data available. This work is partially supported by the sponsors of the Gravity and Magnetics Research Consortium (GMRC): Anadarko, Bell Geospace, BGP, BP, ConocoPhillips, Fugro, Gedex, Marathon Oil, Petrobras, and Vale.

REFERENCES

- Anstie, J., T. Aravanis, P. Johnston, A. Mann, M. Longman, A. Sergeant, R. Smith, F. Van Kann, G. Walker, G. Wells, and J. Winterflood, 2010, Preparation for flight testing the VK1 gravity gradiometer: In R. J. L. Lane (editor), Airborne Gravity 2010 - Abstracts from the ASEG-PESA Airborne Gravity 2010 Workshop: Published jointly by Geoscience Australia and the Geological Survey of New South Wales, Geoscience Australia Record 2010/23 and GSNSW File GS2010/0457.
- Geoscience Australia, 2010, Kauring Airborne Gravity Test Site, <http://www.ga.gov.au/minerals/projects/current-projects/kauring.html>, accessed 16 December 2010.

Hansen, P., 1992, Analysis of discrete ill-posed problems by means of the l-curve: SIAM Review, 34.

